Journal of Cereal Science 63 (2015) 81–87

Contents lists available at ScienceDirect

Journal of Cereal Science

journal homepage: www.elsevier.com/locate/jcs

Real-time 3D visualization and quantitative analysis of internal structure of wheat kernels

Anup Suresh, Suresh Neethirajan*

BioNano Laboratory, School of Engineering, University of Guelph, Guelph, ON, Canada N1G 2W1

ARTICLE INFO

Article history:
Received 24 March 2014
Received in revised form
16 March 2015
Accepted 29 March 2015
Available online 18 April 2015

Keywords:
3D visualization
Sprout damage
Insect damage
Wheat kernels
Micro X-ray CT

ABSTRACT

Food micro-structure plays a crucial role in determining the properties of its end products. Micro X-ray Computer Tomography (CT) provides an excellent tool to assess the internal components of food products non-destructively. This paper describes the 3D visualization and quantitative analysis of the internal features of Canadian Amber Durum Wheat kernel after damage caused by sprouting and insect infestation with *Cryptolestes ferrugineus*. Micro X-ray CT images were reconstructed and processed using image processing algorithms. Imaging techniques such as segmentation and thresholding were used to render visualization modules such as volume rendering, geometric reconstruction, skeletonization and absolute permeability experiment simulation. In addition to visualization, morphometric parameters such as porosity, anisotropy and absolute permeability were determined in a selected region of interest of the sprout damaged and insect infested wheat kernel. Our data revealed that sprouting damage is first evident in the middle section of the sprouted wheat kernel, and associated with greater porosity than the insect damaged kernel. Insect damage occurred on the bottom of the wheat kernel. Compared to sprout damaged kernels, insect damaged kernels had similar anisotropy. X-ray micro CT is a powerful tool for the non-invasive investigation of damage, and microstructure organization in biological materials such as single wheat kernels.

1. Introduction

The microstructural features of food products influence the physical, textural and sensory properties of the end products (Aguilera, 2005). For example, the microstructure of wheat used to manufacture pasta significantly influences the resulting quality and cooking properties of the end product. Investigation of the internal 3-dimensional structural features such as pores, starch granules, protein assemblies and food biopolymer matrices allows for characterization and modeling of the food product parameters in a non-destructive way. The internal structure determines the structure–function relationship, and thus can be used to predict the heat and mass-transfer properties that are relevant to drying, cooking and processing the product (Besbes et al., 2013a).

Wheat kernels have an outer layer of hard tissue called bran surrounding the germ and endosperm layers. As a result, it is difficult to study the internal features, such as structural damage due to insect infestation and early sprouting, without destroying the kernel. The capsule tissue remains intact, but internal cracks are formed in the seed endosperm tissue. During seed development, the air spaces surrounding the germ affect the aerobic respiration of the seed (Verboven et al., 2013), and breaks in the endosperm tissue reduce the nourishment that an embryo or the germ portion can receive. This can negatively impact the vitality of the seeds. The ways that wheat kernels are affected by the various stresses associated with sprouting and insect damage have not been previously characterized. The characteristic locations and directionality of cracks inside a wheat kernel have not been investigated thoroughly before.

Traditional microstructure analysis techniques such as light microscopy (LM) and electron microscopy (EM) and the confocal laser scanning microscopy (CLSM) are only able to yield information regarding the internal structure if the product is cut into cross sections. The sample preparation techniques required by such methods, such as freezing, sectioning, preserving, and staining are

* Corresponding author. School of Engineering, 50 Stone Road East, University of Guelph, Guelph, ON, Canada N1G 2W1. Tel.: +1 519 824 4120x53922; fax: +1 519 836 0227.
E-mail address: sneethir@uoguelph.ca (S. Neethirajan).

http://dx.doi.org/10.1016/j.jcs.2015.03.006
0733-5210/

not only time consuming but likely to disrupt the original structure and introduce imaging artefacts.

Other methods of imaging that also require sectioning, but provide additional information about the chemical and molecular content of the product are Scanning Transmission X-ray Microscopy (STXM) and Synchrotron-powered Fourier transform infrared (FTIR) microspectroscopy. STXM was used to quantify the mineral content localized to the wheat endosperm (Karunakaran et al., 2007). The authors noted that the traditional fixation and resin embedding preparation interfered with the imaging process. In Synchrotron-powered FTIR microspectroscopy, the molecular composition and microstructural features of the wheat showed the distribution of nutrients and carbohydrate structures at a high resolution of 3–10 μm (Yu et al., 2007), which is comparable to the resolution achievable through non-destructive imaging of the micro X-ray computed tomography.

Micro X-ray CT is a powerful tool for non-destructive 3D visualization and characterization of the internal micro-structure of food products at high resolution. Compared to conventional CT scanning, micro CT provides supreme resolution images of small samples such as a single wheat kernel. The SkyScan 1072 system used in this study has a maximum resolution of 4 μm. Morphometric parameters that can be derived from 3D image reconstructions include porosity, anisotropy and absolute permeability of the matrix structures. Porosity, anisotropy and absolute permeability are defined as follows:

- Porosity is the ratio of pore space to the total volume of the sample and is represented in percentage
- Anisotropy is the degree of 3D symmetry ranging between 0 (isotropy) and 1 (anisotropy)
- Absolute permeability is the ability of the sample to transmit a single phase fluid (air or water) through its porous region. It is measured in m^2 or μm^2 and is estimated numerically by Stokes equation

3D rendering has been applied widely to investigate morphological differences in food products due to seed development, strain differences, or evolutionary pressure. In barley, volume changes and tissue development in 18 tissues or tissue complexes were characterized over the course of seed development using 3D reconstruction from digital images of cross sections (Gubatz et al., 2007). Similarly, wheat kernel hardness and the effect of pre-germination on endosperm texture can be determined using X-ray micro CT image analysis. Using X-ray microtomography, different strains of rice can be characterized by differences in starch granule shapes and pore shapes (Van Dalen et al., 2003; Zhu et al., 2012). Furthermore, the microstructural effects of various rice processing techniques has been determined using X-ray micro CT (Mohorič et al., 2009). Micro CT also has a role in comparing the differences between 3000 year old barley, malt, and wheat grains to their modern day equivalents to investigate the evolutionary changes in grain structure (Palmer, 1995).

X-ray microtomography has been widely applied to the analysis of other food products to determine qualities such as internal density and porosity. These qualities can change when bread is baked under different baking conditions (Besbes et al., 2013b), in pans or freestanding structures (Van Dyck et al., 2014), or with the addition of ingredients such as bran to increase fiber content (Van Dyck et al., 2013). These studies examine the microstructural qualities of bread such as molding lines, crust artifacts, and porosity. Bread pores have been noted to be extensively interconnected (Wang et al., 2011) and demonstrate a degree of anisotropy due to pore directionality in bread, possibly resulting in a lack of homogeneity within the loaf (Falcone et al., 2005).

The microstructure of the food can be related to the organoleptic properties such as the crispiness of extruded cereals (Chanvrier et al., 2013). X-ray micro CT has also been employed to compare the drying methods for banana chips in order to determine which cooking methods lead to the greatest porosity (Léonard et al., 2008). Meringues are a classic porous food, and X-ray CT was used to examine the effects of different ratios of ingredients and the effect of fresh ingredients on meringue microstructure (Licciardello et al., 2012). In addition to affecting the texture of the product, pores provide a potential space for enrichment. In apples, larger pores were found near the core, and these can be infused with additives such as quercitin (Schulze et al., 2012). X-ray CT has been used to examine the vessels in plant root structures (Wu et al., 2009), which may be a useful indicator of favorable growth conditions or favorable genetic traits.

In mathematical models of heat and mass transfer in food, models based on macroscale parameters can be enhanced with the addition of microscale modeling information gained from X-ray CT. This multiscale modeling technique increases the quality and applicability of the model. For this purpose, X-ray micro CT analysis is used to determine the microscale properties of the product, which can then be explicitly modeled rather than being incorporated as random effects (Ho et al., 2013). As a result, multiscale modeling provides superior models of heat transfer to corn kernels (Zhang et al., 2013).

Accurate measurement of density at the micron scale, for example the density of wheat kernels, can influence the selection of the ideal food processing protocols and the structural properties of the resulting food product (Kelkar et al., 2011). Similarly, there are several useful 3D reconstruction algorithms for the determination of true density, apparent density and bulk density in food (Kelkar et al., 2011). In algorithms for 3D reconstruction, modeling food products as two-phase random systems is useful for determining the pore distribution, size, and homogeneity. The slowest decay of the linear function of Altamura bread indicated high dimensional inhomogeneity despite having smaller pores than white bread (Derossi et al., 2013).

X-ray CT is useful for detecting the micro-location of internal seed tissue, the moisture dependent properties, and the direction of stress induced cracks. Changes in anisotropy can be used to quantify the formation of directional cracks before cracks are externally visible. Spatial information can be used to determine if cracks initially form between the seed capsule and the endosperm tissue, or elsewhere. The overall goal of our study was to investigate the 3D spatial distribution of the internal microstructure of insect and sprout damaged wheat kernels using X-ray micro CT images. It is crucial to determine the precise internal structure of wheat in order to predict moisture transport and visco-elastic stresses during sorption and drying of wheat grains.

2. Materials and methods

2.1. Sample preparation

Cleaned and sifted samples of Canadian Amber Durum Wheat were randomized to two sample groups. One group was damaged by insect infestation and the other group was damaged by sprouting. The insect infested sample was exposed to *Cryptolestes ferrugineus* (Stephens) larvae. Sprouted samples were prepared as per the protocol by Neethirajan et al. (2007). Briefly, a wheat sample of 50 g was surface-sterilized by soaking in a 2% aqueous sodium hypochlorite solution for 15 min at 24 °C and rinsed with distilled water for about 20 min. The sample was soaked overnight for about 14 h in excess distilled water at 4 °C with one water change. The same sample was again rinsed well with distilled water

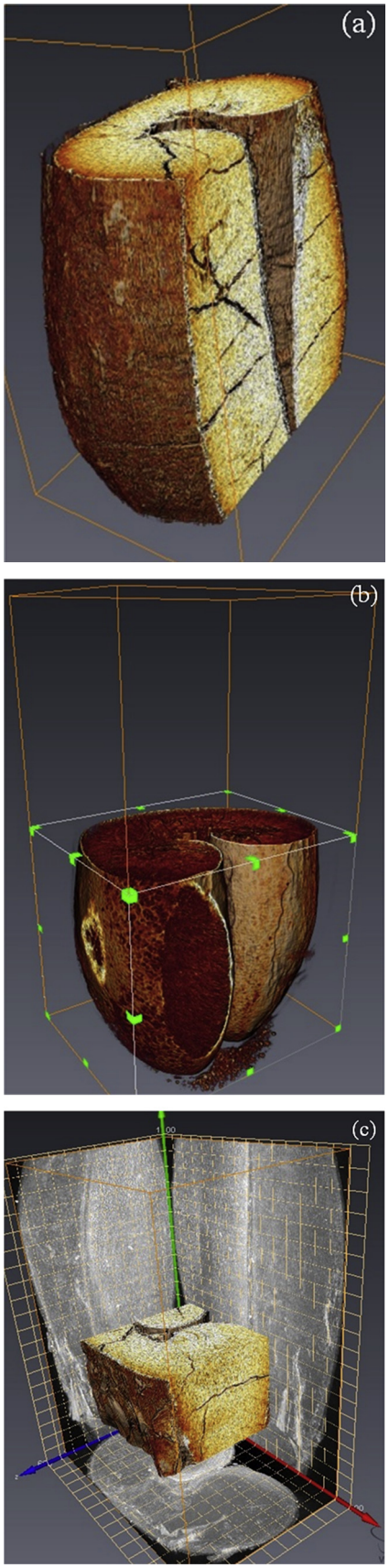

Fig. 1. 3D visualizations of samples by volume rendering. (a) Vertical cross-section of insect infested wheat kernel; (b) horizontal cross-section of sprout damaged wheat kernel; (c) region of interest in the insect infested wheat kernel alongside its ortho-projection.

and was spread on cellulose pads and germinated at 21 °C, 70% relative humidity. After 48 h, the samples were withdrawn and frozen at −30 °C and then freeze dried for about 96 h. Roots and coleoptiles were removed after freeze drying. The freeze dried samples were stored at −5 °C and were ready for scanning as sprouted sample. Another sample of 50 g wheat was surface-sterilized and freeze dried immediately and used as healthy sample.

Infested kernels were prepared by artificial implantation of insect eggs in the germ area of the kernels. *C. ferrugineus* adults were allowed to feed on wheat flour for 24 h at 30 °C and 70% relative humidity (RH). The insect egg was implanted into the kernel through a hole made in the seed coat over the germ using a single hair brush, and followed by placing the kernel in a gelatin capsule for incubation at 30 °C and 70% RH.

2.2. 3D visualization and analysis

3D visualization and quantitative analysis was performed using the Avizo® Fire VSG software (Burlington, USA) along with software extensions XLab Hydro and XSkeleton. Image pre-processing was performed using filters such as 3D median filter and noise reduction techniques. Some modules were developed after converting the image type to a 16-bit data type from the default 8-bit. Simple 3D visualizations were developed using volume rendering and iso-surface rendering modules. Various regions of interest were observed and inner regions of the 3D visualization were developed by extracting a sub-volume and using ortho-projections.

2.3. Absolute permeability experiment simulation

Skeletonization using the XSkeleton extension was performed on three different regions (middle, bottom and top) of the 3D wheat kernel rendering following pre-processing. The skeletonization module displayed the spatial graph of interconnected porous network throughout the kernel. The spatial graph was then converted to a line set module to access additional display tools and parameters. Lastly, an absolute permeability experiment simulation was performed to observe and calculate the absolute permeability through a region of interest within the wheat kernels. Pre-processing techniques were applied followed by segmentation and creation of a label field. Following further processing and quantification, the illuminated streamlines function was used to visualize the velocity flow and a height map slice was used to visualize the pressure field.

2.4. 3D-data generation by X-ray microtomography

2D CT images were collected using the Sky Scan 1172 micro computed tomography scanner (Bruker-MicroCT, Belgium). The X-ray source was operated at 40 kV and 250 μA. Scan exposure times of 1178 ms were used, and 5 frames were averaged for each exposure to reduce noise. CT scanning produced 530 slice images for the insect infested durum wheat kernel with an image resolution of 4.8 × 4.8 × 4.8 μm and 430 slice images for the sprouted durum wheat kernel with an image resolution of 7.8 × 7.8 × 7.8 μm.

2.5. 3D data analysis of pore size distribution

Following observations of 3D modules, a region of interest was selected which was then binarized to convert the gray scale image to a binary image and highlight the porous area within the region of interest. Binarization was performed using segmentation and

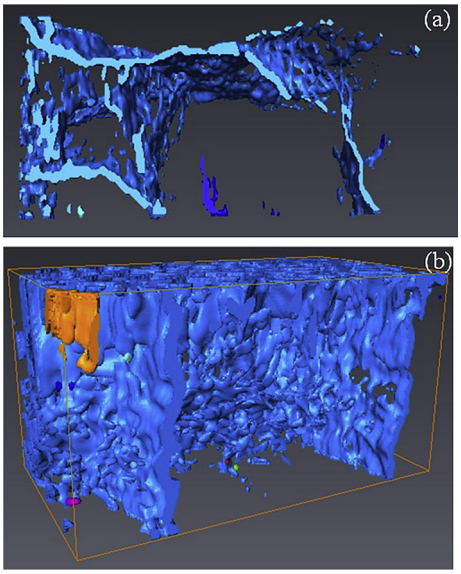

Fig. 2. 3D reconstruction of the porous region in the region of interest of (a) insect infested wheat kernel and (b) sprout damaged wheat kernel.

multi-thresholding techniques. Finally, separation and filtration was applied to obtain distinct pores and eliminate insignificant ones and a 3D geometric surface reconstruction module was simulated to obtain the porosity.

2.6. Statistical analysis

An independent group t-test was done to check the difference between the means of area of pores and the number of pores in the wheat kernel (SAS version 8.2, Statistical Analysis Systems, Cary, NC).

3. Results and discussion

Micro CT images were used to reconstruct 3D renderings of the internal cavities formed by insect or sprouting damage. These images were analyzed for porosity, anisotropy and absolute permeability.

3.1. 3D models volume rendering

Volume rendering is necessary to understand the overall structure of the samples and visualize the internal microstructures. In the cases of direct volume rendering, the entire data sets were loaded. TIFF image scans of the samples ranged from 1 to 2 GB and would have required significant time, or computer processing power. Therefore, reconstruction was performed using 142 MB worth of JPEG CT image scans for the insect infested sample and 73.5 MB of JPEG CT image scans for the sprouted wheat kernel. A region of interest (ROI) box was selected on the 3D volume rendered model to obtain the various horizontal and vertical cross sections. Fig. 1a shows the internal micro-cracks in the vertical cross section of the insect infested wheat kernel. Fig. 1b shows the internal micro-cracks and porous structure in a horizontal cross section of the sprouted wheat kernel bounded by the region of interest (ROI) box. Fig. 1c displays a small cross-sectional volume of the insect infested sample along with its image ortho-projection, helping us identify where the volume of interest lies in the entire volume. The Avizo® Fire software computes the volume rendering by the transmission of light through the volume of the data set with each of the voxels absorbing the necessary color along the way based on the assigned absorption properties.

3.2. 3D geometric reconstruction

Due to the lack of a high-end processing computer, 3D reconstruction of the porous regions in both the samples was rendered on a small ROI. The ROI was selected randomly in a region near the germ of the kernels, where the earliest changes occur. Fig. 2a and b displays the respective regions of interest in the samples reconstructed to view the porous region in 3D and obtain the porosity and anisotropic degree (Table 1). As summarized in Table 1, sprouting damage was associated with greater porosity than the insect damage, but there was not a large difference in anisotropy.

3.3. Skeletonization

With the use of Avizo® Fire extension XSkeleton, we were able to render the skeletonized model of samples. The software computes the model by generating points called nodes at every porous region and interconnecting these nodes by lines called segments. A 3D spatial distribution of the porous network within the samples was generated. Due to the high computational requirement, the kernels were split into three different regions (bottom, middle and top) using the X-ray micro CT images. The skeletonization models for each of these regions were rendered separately but with similar parameters, and were then superimposed to one image for better viewing. Fig. 3a and b shows the three different skeletonized regions (top, middle, and bottom) of insect infested and sprouted durum wheat kernels, respectively. Graphs in Fig. 3c and d display a comparative analysis of the morphometric parameters in the three different regions of insect damaged and sprout damaged kernels respectively.

3.4. Absolute permeability experiment simulation

For the calculation of absolute permeability, the XLab Hydro extension was used. The software sets up the experiment in a way such that only 2 opposite faces of a cube (ROI) are left open while the other 4 sides and pressure and velocity are applied through one side of the volume and the flow is observed. The input pressure, output pressure and the flow rate are kept constant and the absolute permeability is calculated. The software generates a pressure file representing the scalar pressure field and velocity file representing the velocity vector field. Fig. 4a and c shows the height map slice and volume rendering (representing the pressure field) and 4b shows the illuminated streamlines (representing the

Table 1
Morphometric parameters of insect infested and sprout damaged wheat kernels in a region of interest (ROI).

Grain type	Porosity	Anisotropic degree	Lattice size (ROI)
Insect infested durum wheat kernel	0.22	0.55	124 × 125 × 265
Sprout damaged durum wheat kernel	1.74	0.58	128 × 230 × 128

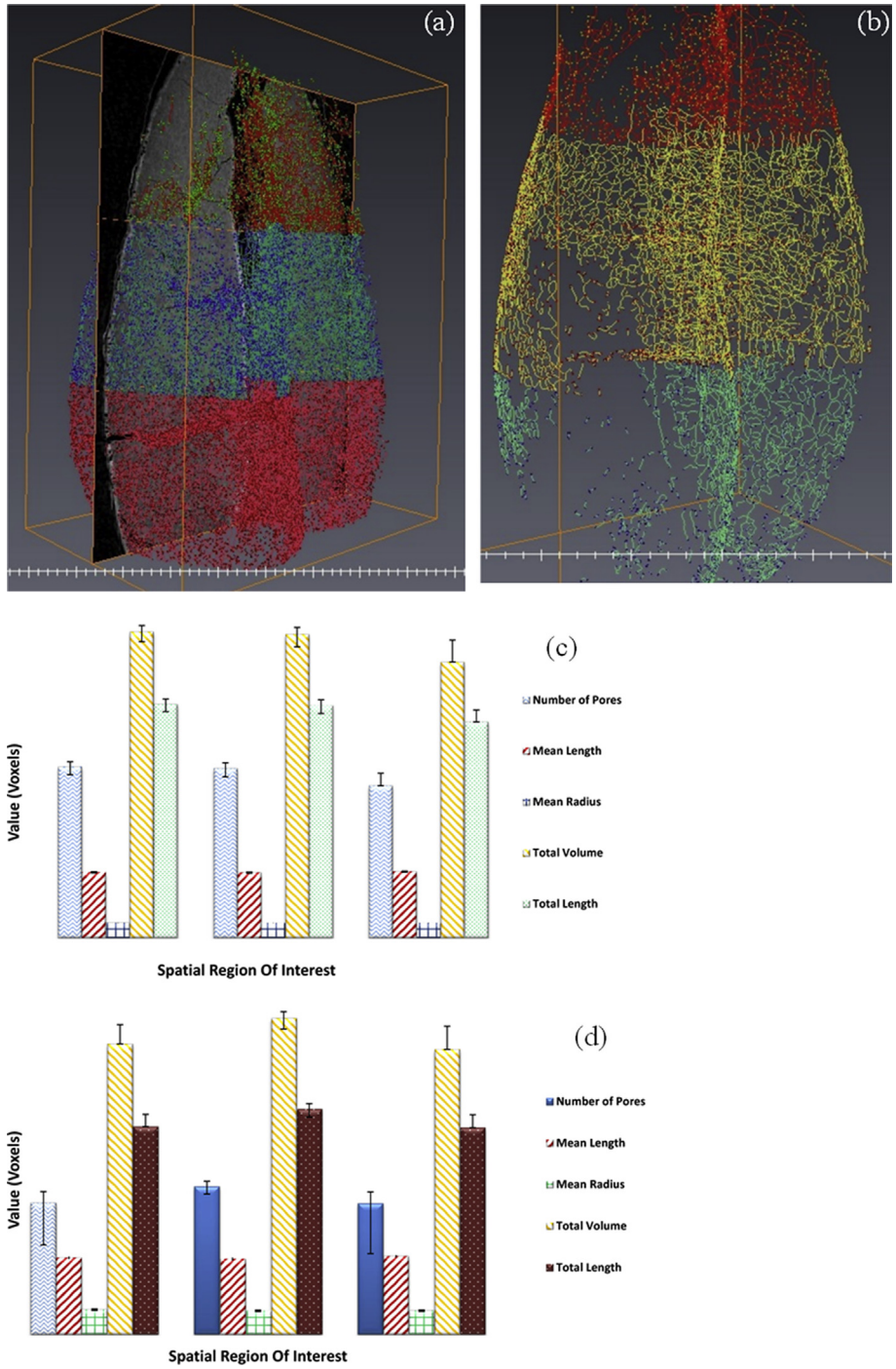

Fig. 3. 3D skeletonization models of bottom, middle and top Portions of the wheat kernels displaying the nodes and segments. (a) Skeletonization of insect infested wheat kernel along with an ortho-slice in the middle; (b) skeletonization of sprouted wheat kernel along with an ortho-slice in the middle; (c) graph comparing morphometric parameters between three regions of the skeletonized model from insect infested wheat kernel in (a); (d) graph comparing morphometric parameters between 3 regions of the skeletonized model from sprouted wheat kernel in (b).

velocity field) of a ROI in the insect damaged kernel. Fig. 4d–f displays similar representations of a ROI in the sprouted wheat kernel. Higher to lower intensity regions are represented as colors red to blue, in the web version. The sprout damaged wheat kernel simulation showed a well distributed network of channels for fluid flow, which is consistent with the greater porosity. The insect damaged wheat kernel had higher pressures and fewer larger channels for flow.

3.5. Fissure propagation mechanism

The non-invasive 3-dimensional tomographic imaging for detailed insight of small fissure evolutions in the range of microns was observed using the X-ray micro CT images. The fissure or the crack growth analysis of insect damaged kernel shows that the path is tortuous in nature with multiple branching. Tunneling was pronounced, indicating that the cracks and the fissures are strongly

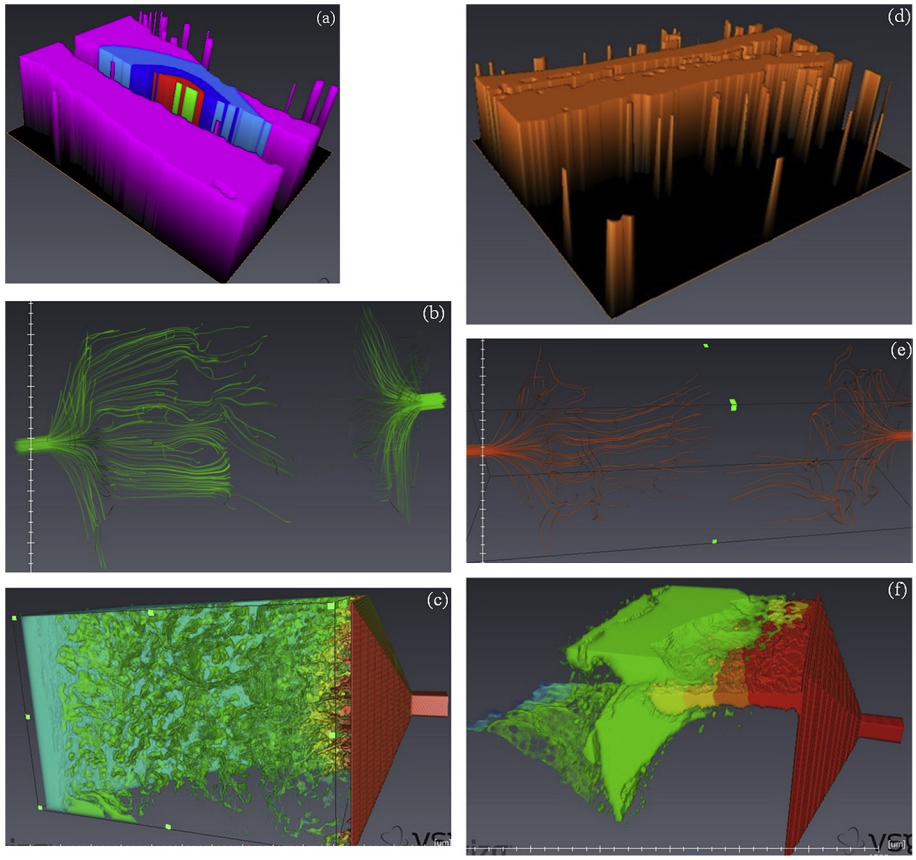

Fig. 4. Results of absolute permeability experiment simulation of insect damaged wheat kernel as a height map slice (a), illuminated streamlines (b), volume rendering (c); results of absolute permeability experiment simulation of sprout damaged wheat kernel as a height map slice (d), illuminated streamlines (e), volume rendering (f).

micro-structure dependent. The differences between germinating seed and insect damaged seed is because the former has gone through an extensive physiological process while the latter is basically due to physical damage.

4. Conclusions

High contrast micro X-ray CT imaging was employed to compare internal wheat kernel damage due to sprouting and insect damage. Analysis of the cracks in the insect damaged kernels showed that the path is tortuous with multiple branching. Morphometric internal pore-network analysis reveals that the 3D anisotropic degree is nearly the same for all cross sections in both samples. Porosity was higher in the sprout damaged kernels than in the insect infested kernels. In sprout damaged kernels, pore volume is highest in the middle region, whereas in the case of insect infested kernels, pore volume is highest in the bottom region. The calculated quantitative information can be used as input for simulation models for moisture diffusion. In fluid flow simulations, the sprout damaged wheat kernel simulation showed a well distributed network of channels for fluid flow, which is consistent with the greater porosity. In contrast, the insect damaged wheat kernel had higher pressures and fewer larger channels for flow.

Acknowledgments

The authors thank the Natural Sciences and Engineering Research Council of Canada, the Canada Foundation for Innovation, the Ontario Ministry of Research and Innovation, and the Ontario Ministry of Food and Agriculture for funding this study.

References

Aguilera, J.M., 2005. Why food microstructure? J. Food Eng. 67, 3–11.
Besbes, E., Jury, V., Monteau, J.Y., Le Bail, A., 2013a. Water vapor transport properties during staling of bread crumb and crust as affected by heating rate. Food Res. Int. 50, 10–19.
Besbes, E., Jury, V., Monteau, J.Y., Le Bail, A., 2013b. Characterizing the cellular structure of bread crumb and crust as affected by heating rate using X-ray microtomography. J. Food Eng. 115, 415–423.
Chanvrier, H., Jakubczyk, E., Gondek, E., Gumy, J.C., 2013. Insights into the texture of extruded cereals: structure and acoustic properties. Innov. Food Sci. Emerg. 24, 61–68.
Derossi, A., Pilli, T., Severini, C., 2013. Statistical description of food microstructure. Extraction of some correlation functions from 2D images. Food Biophys. 8, 311–320.
Falcone, P.M., Baiano, A., Zanini, F., Mancini, L., Tromba, G., Dreossi, D., Montanari, F., Scuor, N., Nobile, M.A.D., 2005. Three-dimensional quantitative analysis of bread crumb by X-ray microtomography. J. Food Sci. 70, E265–E272.
Gubatz, S., Dercksen, V.J., Brüß, C., Weschke, W., Wobus, U., 2007. Analysis of barley (*Hordeum vulgare*) grain development using three-dimensional digital models: 3D digital models of developing barley grains. Plant J. 52, 779–790.
Ho, Q.T., Carmeliet, J., Datta, A.K., Defraeye, T., Delele, M.A., Herremans, E., Opara, L., Ramon, H., Tijskens, E., van der Sman, R., Van Liedekerke, P., Verboven, P., Nicolaï, B.M., 2013. Multiscale modeling in food engineering. J. Food Eng. 114, 279–291.
Karunakaran, C., Gaillard, C., Bouchet, B., Gnaegi, H., Buleon, A., Wang, J., Hitchcock, A.P., 2007. Characterization of Wheat Grain Tissues by Soft X-Ray Spectromicroscopy. Canadian Light Source Inc, Saskatoon.
Kelkar, S., Stella, S., Boushey, C., Okos, M., 2011. Developing novel 3D measurement techniques and prediction method for food density determination. Procedia Food Sci. 1, 483–491.
Léonard, A., Blacher, S., Nimmol, C., Devahastin, S., 2008. Effect of far-infrared radiation assisted drying on microstructure of banana slices: an illustrative use of X-ray microtomography in microstructural evaluation of a food product. J. Food Eng. 85, 154–162.
Licciardello, F., Frisullo, P., Laverse, J., Muratore, G., Del Nobile, M.A., 2012. Effect of sugar, citric acid and egg white type on the microstructural and mechanical properties of meringues. J. Food Eng. 108, 453–462.

Mohorič, A., Vergeldt, F., Gerkema, E., Dalen, G. van, Doel, L.R. van den, Vliet, L.J. van, As, H.V., Duynhoven, J. van, 2009. The effect of rice kernel microstructure on cooking behaviour: a combined μ-CT and MRI study. Food Chem. 115, 1491–1499.

Neethirajan, S., Jayas, D.S., White, N.D.G., 2007. Detection of sprouted wheat kernels using soft X-ray image analysis. J. Food Eng. 81, 509–513.

Palmer, G.H., 1995. Structure of ancient cereal grains. J. Inst. Brew. 101, 103–112.

Schulze, B., Peth, S., Hubbermann, E.M., Schwarz, K., 2012. The influence of vacuum impregnation on the fortification of apple parenchyma with quercetin derivatives in combination with pore structures X-ray analysis. J. Food Eng. 109, 380–387.

Van Dalen, G., Blonk, H., van Aalst, H., Hendriks, C.L., 2003. 3-D imaging of foods using X-ray microtomography. GIT Imaging Microsc. 3, 18–21.

Van Dyck, T., Verboven, P., Herremans, E., Defraeye, T., Van Campenhout, L., Wevers, M., Claes, J., Nicolaï, B., 2014. Characterisation of structural patterns in bread as evaluated by X-ray computer tomography. J. Food Eng. 123, 67–77.

Van Dyck, T., Verboven, P., Wevers, M., Claes, J., Nicolai, B., 2013. Imaging and characterisation of microstructural heterogeneity in bread. In: Proceedings of the 1st International Conference on Tomography of Materials and Structures. International Conference on Tomography of Materials and Structures. Ghent, Belgium, 1–5 July 2013.

Verboven, P., Herremans, E., Borisjuk, L., Helfen, L., Ho, Q.T., Tschiersch, H., Fuchs, J., Nicolaï, B.M., Rolletschek, H., 2013. Void space inside the developing seed of *Brassica napus* and the modelling of its function. New. Phytol. 199, 936–947.

Wang, S., Austin, P., Bell, S., 2011. It's a maze: the pore structure of bread crumbs. J. Cereal Sci. 54, 203–210.

Wu, H., Jaeger, M., Wang, M., Li, B., Zhang, B.G., 2009. Three-dimensional reconstruction and visualization of xylem vessels of wheat nodal root. In: Plant Growth Modeling, Simulation, Visualization and Applications (PMA), 2009 Third International Symposium. IEEE.

Yu, P., Block, H., Niu, Z., Doiron, K., 2007. Rapid characterization of molecular chemistry, nutrient make-up and microlocation of internal seed tissue. J. Synchrotron Radiat. 14, 382–390.

Zhang, S., Kong, N., Zhu, Y., Zhang, Z., Xu, C., 2013. 3D model-based simulation analysis of energy consumption in hot air drying of corn kernels. Math. Probl. Eng. 2013, 1–12.

Zhu, L.J., Dogan, H., Gajula, H., Gu, M.H., Liu, Q.Q., Shi, Y.C., 2012. Study of kernel structure of high-amylose and wild-type rice by X-ray microtomography and SEM. J. Cereal Sci. 55, 1–5.